New Journal of Physics
The open–access journal for physics

Magnetic field generation by coherent turbulence structures

D Kivotides, A J Mee and C F Barenghi[1]
School of Mathematics, University of Newcastle, Newcastle-upon-Tyne NE1 7RU, UK
E-mail: c.f.barenghi@ncl.ac.uk

New Journal of Physics **9** (2007) 291
Received 4 December 2006
Published 31 August 2007
Online at http://www.njp.org/
doi:10.1088/1367-2630/9/8/291

Abstract. It is thought that the small-scale magnetic fields observed in accretion discs, galaxies and galactic clusters are generated by a dynamo process in which the turbulent plasma amplifies small initial magnetic fluctuations. Numerical simulations of turbulence have revealed that turbulence consists of filament-like vortex structures superimposed on an incoherent background, which carry a considerable amount of the energy. The natural questions to ask are whether these coherent structures can generate a magnetic field and, if so, if the generated magnetic field is also filament-like. After setting up a turbulence model which consists only of vortex filaments, we show in an unambiguous way that the coherent structure can sustain kinematic dynamo action and that the magnetic field thus generated consists of relatively thick ribbons (flattened tubes) located in between vortices.

[1] Author to whom any correspondence should be addressed.

PII: S1367-2630(07)38841-1

Contents

1. Introduction

The origin of the fluctuating, or small-scale turbulent magnetic fields observed in the solar photosphere, accretion discs, galaxies and galactic clusters is a fundamental problem of astrophysics. It is thought that in these systems the magnetic field is generated by a dynamo process [1, 2]. In this process, the three-dimensional turbulent velocity field of the constituent plasma amplifies small initial magnetic fluctuations by stretching existing field lines and overcoming ohmic dissipation until nonlinear saturation is achieved by the back-reaction of the Lorentz force on the turbulent velocity field. The dynamo problem thus consists of two distinct aspects [3]. The first is the kinematic dynamo, in which one asks if the magnetic field grows or decays exponentially in the presence of a prescribed velocity field; the second refers to the nonlinear saturation. This paper is concerned with the first aspect. Understanding the turbulent dynamo, even only at kinematic level, requires a sufficiently good model of turbulent flows. In recent years, numerical simulations have revealed that homogeneous isotropic turbulence is dynamically dominated by metastable coherent vortex structures, a network of mini-tornadoes called vortex tubes or filaments [4]–[7]. The coherent structures have a linear dimension comparable to the system size, and are superimposed on an incoherent velocity background. More careful analysis [8] has suggested that the coherent structures carry a considerable amount of the energy and the enstrophy of the turbulence and correspond to the observed Kolmogorov spectrum of the total (coherent plus incoherent) velocity field. It seems [9] that the apparently chaotic behaviour of turbulent flow is due to the nonlinear interactions of coherent vorticity structures, which also create a small-scale velocity field which is dissipated at the smallest scales by viscous forces. As pointed out by Zeldovich *et al* [1], a fundamental question arises: 'In a linear hydromagnetic problem, the behaviour of the magnetic field is considered against the background of independently prescribed velocity field. The existence of velocity fields with vortex filaments gives rise to interesting problems as regards to the behaviour of the magnetic field in such flow. Will magnetic ropes arise from this velocity field? Will the ropes coincide with the vortex lines?' Our aim is to answer this simple kinematic question, as well as to clarify related issues such as the scaling of the magnetic energy spectrum and the nature of the stretching of magnetic field lines by turbulent strain.

A straightforward method for answering such questions is to solve numerically the Navier–Stokes equation in order to create the turbulence which drives a dynamo [10, 11]. At present however, there are no pattern recognition methods powerful enough to define unambiguously the coherent vorticity structures and follow their motion and interactions in time. In addition, even if such methods were available, a significant part of the computational effort would still

had to be devoted to the computation of the dynamics of incoherent vorticity and so there is a limit on the Reynolds number that could be achieved in practice. Therefore studies of vortex dynamos were based on suitable models. One approach [12] used an idealized two-and-a-half dimensional turbulent velocity field mode and showed that most of the stretching of magnetic field lines takes place between vortex patches. Another approach consisted of Herzenberg-type rotors, used to numerically mimic vortex tubes [13]. In this paper, we introduce a different method of investigation that allows the explicit representation of three-dimensional coherent vorticity in homogeneous isotropic turbulence.

2. Model

Our model of turbulence is based solely on three-dimensional, reconnecting vortex filaments with dynamic finite cores of uniform circulation which interact via inertial and viscous forces [9, 14, 15]. In this way, the turbulent velocity field contains only the coherent vortex structure, whose effect on the magnetic field generation we wish to investigate; the incoherent part of the turbulence is neglected. Essentially, our investigation is not a direct numerical calculation of the turbulent velocity field, but a calculation of the dynamics of vortex filaments in an incompressible fluid, whose configuration at a particular instant allows the reconstruction of a homogeneous and isotropic turbulent velocity field. The position $\mathbf{r}(s, t)$ of the centreline of each filament moves according to $\mathrm{d}\mathbf{r}/\mathrm{d}t = \mathbf{V}(\mathbf{r}, t)$ where t is time, s is arc length measured along the filament, and the velocity field $\mathbf{V}(\mathbf{r}, t)$ is given by the Biot–Savart law [16]

$$\mathbf{V}(\mathbf{r}, t) = -\frac{1}{4\pi} \int \frac{(\mathbf{r} - \mathbf{r}') \times \boldsymbol{\omega}(\mathbf{r}')\, \mathrm{d}\mathbf{r}'}{|\mathbf{r} - \mathbf{r}'|^3}, \tag{1}$$

where the integral is performed along all vortex filaments. If the vorticity distribution $\boldsymbol{\omega}(\mathbf{r}, t)$ were a delta-function concentrated in the core, this formula would state that a vortex filament at a point simply moves in the binormal direction with speed inversely proportional to the local radius of curvature at that point [17]. In our model $\boldsymbol{\omega}(\mathbf{r}, t)$ is proportional to the circulation Γ and is a Gaussian function [9] which peaks along the centreline $\mathbf{r}$. The radius of the vortex tube, σ, is defined as the standard deviation of this Gaussian distribution; it decreases because of vortex stretching and increases because of viscous diffusion. Numerically, each vortex filament is discretized into a variable number of segments, N, which evolve in time under the action of the Biot–Savart law and viscous forces. The length of the filaments, as well as the number of segments N, increases due to vortex stretching. By construction, outside the vortex core regions, the flow is thus effectively potential. The time stepping of equation (1) is based on a low-storage, third-order Runge–Kutta scheme. The filaments are allowed to reconnect as in [18]. The reconnection procedure introduces an effective viscosity in our computation. In particular, every reconnection locally stretches the filaments and introduces a cascade of energy to smaller scales [19]. The reconnection algorithm [18] damps this cascade; our model is thus akin to a large eddy simulation (LES) method but in vorticity space. However, the molecular viscosity ν remains dynamically significant since it directly affects the tube-radius dynamics of most parts of the vortex tangle that do not participate, at a particular instant of time, in a reconnection. Note also that large-scale consequences of reconnections are taken into account [18] through the generation and propagation of Kelvin waves (see figures 1, 4 and 7 of [18]). Computations performed with

the coherent structures model compare well with properties of turbulence computed by directly solving the Navier–Stokes equation, for example the Kolmogorov scaling of the energy spectrum and the third-order longitudinal structure function [9]. The model also reproduces finer details of Navier–Stokes turbulence like the qualitatively correct statistics of the relative directions of the eigenvectors of the rate of strain matrix and both material line vector and vorticity vector [14].

The magnetic field $\mathbf{B}$ is determined by

$$\frac{\partial \mathbf{B}}{\partial t} = \eta \nabla^2 \mathbf{B} + \nabla \times (\mathbf{V} \times \mathbf{B}), \tag{2}$$

and $\nabla \cdot \mathbf{B} = 0$ where η is the magnetic diffusivity of the plasma. Following the usual kinematic dynamo approach [3], we ask whether, given $\mathbf{V}$, the magnetic field $\mathbf{B}$ grows or not, where the initial condition for $\mathbf{B}$ is a uniform field with (dimensionless) magnetic energy of the order of 10^{-9}. This approach is valid in the early stage of development of $\mathbf{B}$ when $\mathbf{B}$ is small and the back-reaction of $\mathbf{B}$ on $\mathbf{V}$ (which is quadratic in $\mathbf{B}$) can be neglected. The dimensionless driving parameter of the dynamo is the magnetic Reynolds number $Re_\mathrm{m} = Vb/\eta$ where V is the velocity scale and b the length scale. Since in our kinematic dynamo approach we hold the turbulent velocity field fixed, the hydrodynamic Reynolds number $Re = Vb/\nu$ is fixed, and we vary the magnetic Reynolds number by changing the magnetic Prandtl number $Pr_\mathrm{m} = Re_\mathrm{m}/Re = \nu/\eta$.

Equation (2) is solved using a finite difference method on a 256^3 grid. The discretization of the derivatives is second-order in space. The time-stepping is a low storage third-order Runge–Kutta scheme with operator factorization of the Laplacian, and the solenoidal condition is enforced by projecting at each time step the magnetic field on to the space of divergence free vector fields. The volume of fluid which we consider has cubic dimension $b = 1\,\mathrm{m}$; the fluid has kinematic viscosity $\nu = 10^{-4}\,\mathrm{m^2\,s^{-1}}$ and the vortices have circulation $\Gamma = 1\,\mathrm{m^2\,s^{-1}}$. The dynamical equations and the various physical quantities are made dimensionless using b as unit of length and b^2/Γ as unit of time. The employed boundary conditions for both vortices and magnetic field are periodic.

3. Results

To produce the turbulence, we start with an arbitrary number of vortex loops set at random locations and orientations. The loops evolve under the effect of their mutual interaction and undergo a large number of reconnections, quickly forming a time-dependent turbulent tangle. The time step is typically 0.0005 and is determined by the smallest ratio of the tube area over the circulation. After a time of the order of the turnover time τ_l of the largest turbulence eddies in the box ($\tau_\mathrm{l} \approx 0.25$), the turbulent velocity field reaches a statistically isotropic and homogeneous state. Figure 1 shows the vortex filaments (in red). At $t = 0.05$ the total length of the filaments is $L = 58.84$, the number of discretization segments is $N = 3793$ and the average radius of the vortex tubes is $\langle\sigma\rangle = 0.054$. Moreover, 1127 vortex reconnections have occurred in the system. The Reynolds number of the turbulent flow can be defined simply as $Re = \Gamma/\nu = 10\,000$. This estimate is in order-of-magnitude agreement with the value obtained by computing the root mean square value $V = \sqrt{\langle \mathbf{V} \cdot \mathbf{V} \rangle/3}$ of the turbulent fluctuating velocity $\mathbf{V}$, which yields $Re = Vb/\nu \approx 20\,000$. Using the well known [20] relation for homogeneous isotropic turbulence $\lambda/b = \sqrt{15}Re^{-1/2}$, where λ is the Taylor microscale, one finds $Re_\lambda = 548$.

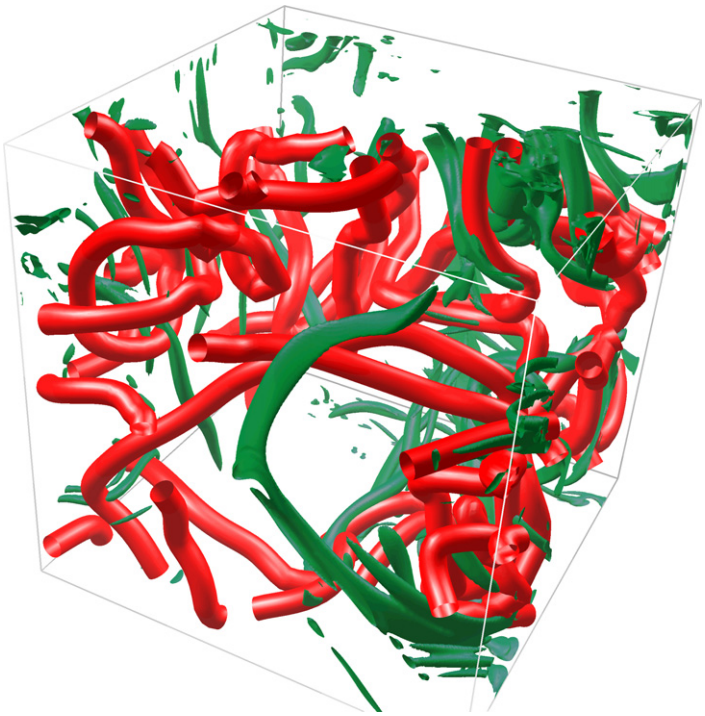

Figure 1. The red tubes represent the coherent vortex structures; for clarity only a fraction (0.7) of the actual vortex tube radii is shown. The green structures are isosurfaces of $|\mathbf{B}|$ at level equal to three times the root mean square value in the box, and represent regions of intense magnetic energy. Note that the magnetic structures are located between the vortex structures and are more ribbon-like flattened tubes rather than rope-like. Time is $t = 2.690$ and $Pr_{\mathrm{m}} = 0.4$.

Figure 2 shows the kinetic energy spectrum

$$E_{\mathrm{K}} = \frac{1}{\mathcal{V}} \int \frac{1}{2} |\mathbf{V}|^2 \, \mathrm{d}^3\mathbf{r} = \int_0^\infty E_{\mathrm{K}}(k) \, \mathrm{d}k, \tag{3}$$

where E_{K} is the kinetic energy, $\mathcal{V} = b^3$ and $k = |\mathbf{k}|$ is the magnitude of the three-dimensional wavevector; it is apparent from the figure that $E_{\mathrm{K}}(k)$ obeys the Kolmogorov $k^{-5/3}$ scaling (solid line at the left), in agreement with [9]. Our turbulence model has no overall rotation or density stratification, so the only helicity is due to small fluctuations; a single vortex filament has velocity $\mathbf{V}$ which is perpendicular to the vorticity $\boldsymbol{\omega}$ of the filament at that point, but the presence of a finite number of other filaments induces perturbations of $\mathbf{V}$ which do not cancel each other out. The resulting helicity is however small; its space-averaged value is $\langle \boldsymbol{\omega} \cdot \mathbf{V} \rangle = 5.426$, whereas the root mean square of the fluctuating velocity is $V = \sqrt{\langle \mathbf{V} \cdot \mathbf{V} \rangle / 3} = 1.935$ and that of the fluctuating vorticity is $\omega = \sqrt{\langle \boldsymbol{\omega} \cdot \boldsymbol{\omega} \rangle / 3} = 31.654$.

Once the turbulence is well developed, we hold $\mathbf{V}$ constant in time, thus freezing the turbulent structures. There are two reasons for this. Firstly, lacking a continual forcing, the turbulence would decay in time due to viscous effects, so we would attempt to create a dynamo driven by a decaying velocity field which would not allow a precise definition of magnetic Reynolds number. Secondly, freezing the turbulence is numerically convenient. The solution of equation (2)

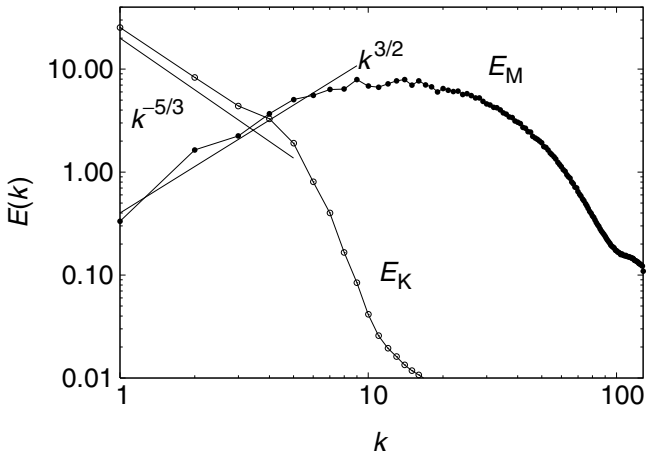

Figure 2. Kinetic energy spectrum $E_K(k)$ and magnetic energy spectrum $E_M(k)$ at time $t = 2.690$ and $Pr_m = 0.4$ plotted versus wavenumber magnitude, $k = |\mathbf{k}|$. The solid lines are the power-laws $k^{-5/3}$ (left) and $k^{3/2}$ (right).

for **B** requires **V** at each point of the 256^3 grid; each of these point then requires the evaluation of Biot–Savart integrals taking into account all vortex segments in the system, and the computational cost of this operation is proportional to N^2.

Figure 3 shows the magnetic energy E_M, versus time for different values of Pr_m. Although for very small Prandtl numbers, $Pr_m = 10^{-8}$, the seed magnetic energy decays, for Pr_m sufficiently large, after an initial transient, there is exponential growth. This proves that the coherent turbulent structures are capable of magnetic field generation. For example, at $Pr_m = 0.003$ the dynamo is in a marginal state and at $Pr_m = 0.01$ we have definitively dynamo action (the corresponding magnetic Reynolds number is $Re_m = Re\,Pr_m = 100$). Since the turbulent velocity field which we use to drive the dynamo is frozen, regions favouring magnetic field growth remain so throughout the calculation, which would not be the case if the filaments could change their positions with time. Thus our estimate of the critical magnetic Reynolds number may be optimistic. On the other hand, Ponty *et al* [21] get dynamos at Pr_m as low as 0.01, so it is not a big disagreement, considering also that we have a different velocity field. Although a series of computations for various magnetic Reynolds numbers were performed, the following discussion of magnetic field structures and spectra, as well as strain–field interactions, refers to the case $Pr_m = 0.4$.

To understand the nature of the turbulent dynamo action we compute the magnetic energy spectrum

$$E_M = \frac{1}{\mathcal{V}} \int \frac{1}{2} |\mathbf{B}|^2 \mathrm{d}^3\mathbf{r} = \int_0^\infty E_M(k)\, \mathrm{d}k, \tag{4}$$

figure 2, which can be compared to the kinetic energy spectrum $E_K(k)$. It is apparent that the energy of the magnetic field is concentrated at higher wavenumbers; the solid line at the right shows that the magnetic spectrum follows the scaling $E_M(k) \sim k^{3/2}$, in agreement with [10] and the Kazantsev model [22]–[24]. The magnetic spectrum peaks at the right of the velocity spectrum, despite the fact that $Pr_m < 1$. This is because due to the reconnection model, the

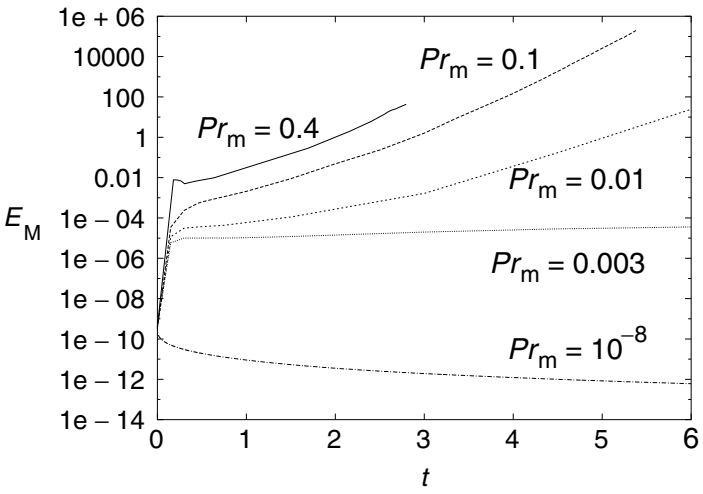

Figure 3. Magnetic energy E_M versus time t respectively for $Pr_m = 0.003, 0.01, 0.1$ and 0.4 (from bottom to top).

smallest scale of the velocity spectrum is not the viscous scale but a scale well inside the inertial range. There is a second dissipation process in the system (induced by the reconnection model) not accounted for by the molecular viscosity. One could make a heuristic estimate of the *effective* (as opposed to molecular) Pr_m in the calculation by using the scaling relation $l_\eta = l_{\nu'}/\sqrt{Pr'_m}$, where $Pr'_m = \nu'/\eta$ is the magnetic Prandtl number based on an effective viscosity ν', and $l_{\nu'}$, l_η are the smallest resolved flow scale and resistive magnetic scale respectively. We find $Pr'_m \approx (20/7)^2 \approx 8$. Following [11], we also compute the eigenvalues Λ_1, Λ_2 and Λ_3 (defined such that $\Lambda_1 > \Lambda_2 > \Lambda_3$) and the corresponding eigenvectors $\mathbf{\Lambda}_1$, $\mathbf{\Lambda}_2$ and $\mathbf{\Lambda}_3$ of the rate of strain matrix defined as $S_{ij} = (1/2)(\partial V_i/\partial x_j + \partial V_j/\partial x_i)$ $(i, j = 1, 2, 3)$ where v_i and x_i are the Cartesian components of $\mathbf{V}$ and $\mathbf{r}$. We find that $\langle\Lambda_1\rangle = 23.284$, $\langle\Lambda_2\rangle = 0.482$, whereas $\langle\Lambda_3\rangle = -23.766$. Note that $\langle\Lambda_1\rangle + \langle\Lambda_2\rangle + \langle\Lambda_3\rangle = 0$ due to the incompressibility of the flow. These results agree qualitatively with fully resolved Navier–Stokes calculations since there also the intermediate eigenvalue has a positive mean value [14, 25]. The angles between the generated magnetic field $\mathbf{B}$ and each eigenvector $\mathbf{\Lambda}_i$ are given by the magnitude of the directional cosines $g_i = |(\mathbf{B}\cdot\mathbf{\Lambda}_i)/|\mathbf{B}||\mathbf{\Lambda}_i|)|$ $(i = 1, 2, 3)$. Histograms of g_i show that the magnetic field tends to align mostly (and consequently to be stretched predominantly by) the first eigenvector of the strain matrix, and to be normal to the third (compressive) eigenvector. There was no distinctive alignment tendency with respect to the intermediate eigenvector. This behaviour is similar to the behaviour of material lines in turbulence [14, 25, 26]. According to these results, it is expected that the magnetic field structures must be ribbon-like, since the magnetic field is stretched, on average, along two directions but the stretching along the $\mathbf{\Lambda}_1$ direction is much stronger than the stretching along the $\mathbf{\Lambda}_2$ direction. In addition, since the field does not prefer to align with $\mathbf{\Lambda}_3$, the ribbon-like structures would not be predominantly flat but instead retain a certain degree of thickness.

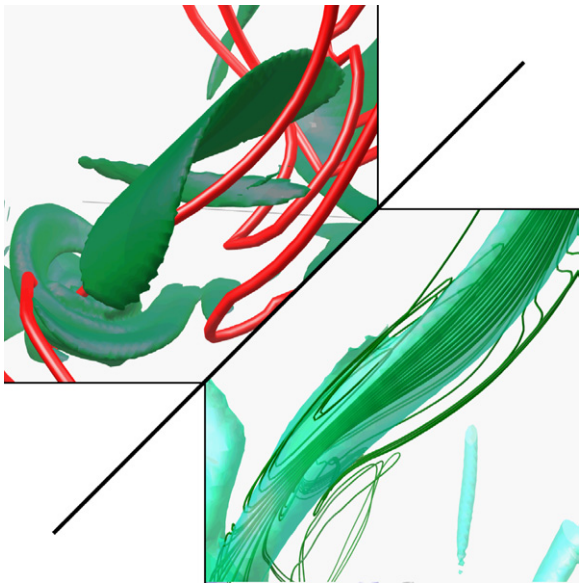

Figure 4. Left: the region of intense magnetic field (in green) wraps around the vortex filament (in red), and is flat and ribbon-like rather than rope-like. The time and magnetic Prandtl numbers are as for figure 1. The magnetic isosurfaces are plotted at the level equal to three times the root mean square value in the box, and the tubes are plotted with a radius equal to $0.005 \approx 0.1\langle\sigma\rangle$. Note that the twisted magnetic sheet structure sits just outside the actual tube radius σ. The graph is a small subsection of the unit box whose size is approximately 0.35 times the full size of the computational domain. Right: example of small-scale magnetic field reversals in a flux tube ($t = 0.635$). These are hinted by the observed peak of the magnetic energy spectrum at high wavenumbers.

4. Discussion

Numerical solutions of the Navier–Stokes equation show that high Reynolds number flows are characterized by metastable coherent vortex structures. Our new model of turbulence, which satisfies the most important properties of the statistical phenomenology of the Navier–Stokes equation, consists only of these coherent structures. This allows us to determine the effect of the coherent vortex structures on the magnetic field generation in an unambiguous way: we show that kinematic dynamo action is indeed possible. Figure 1 shows the magnetic field structures (in green) created by the turbulent vortex filaments (in red). The regions of large magnetic energy tend to be positioned between the vortex filaments. Contrary to the conjecture of Zeldovich *et al* [1], we find no magnetic ropes, but rather relatively thick ribbon-like structures, which occasionally spiral around the filaments, as shown in figure 4 (left), in agreement with what is conjectured in [10]. Small-scale magnetic field reversals are also visible.

Having introduced a new model of turbulence (based on vortex tubes), it was sensible to tackle the kinematic dynamo problem first. Further work will attempt to improve the model and allow the study of the full, dynamically self-consistent dynamo, which includes the back-reaction of the Lorentz force on the velocity field which has generated the magnetic field in the first place. This back-reaction may change the geometry of the magnetic structures which we

have discussed, of course. Further work with more computational power would also allow the study of the time dependence and a wider separation of scales between the viscous scale and the ohmic scale. In the current calculation the effective magnetic Prandtl number is $Pr'_{\rm m} \approx 8$; in this magnetic Prandtl number regime, our results agree with the findings of [10], with the advantage that we deal only and directly with the coherent structures of turbulence.

5. Acknowledgment

The research of DK and CFB is supported by EPSRC grants GR/T08876/01 and EP/D040892/1.

References

[1] Zeldovich Ya B, Ruzmaikin A A and Sokoloff D D 1990 *The Almighty Chance* (Singapore: World Scientific) p 215
[2] Brandenburg A and Subramanian K 2005 *Phys. Rep.* **417** 1
[3] Moffatt H K 1978 *Magnetic Field Generation in Electrically Conducting Fluids* (Cambridge: Cambridge University Press)
[4] She Z S and Orszag S A 1990 *Nature* **344** 226
[5] Jimenez J and Wray A A 1993 *J. Fluid Mech.* **255** 65
[6] Siggia E D 1981 *J. Fluid Mech.* **107** 375
[7] Vincent A and Meneguzzi M 1994 *J. Fluid Mech.* **258** 245
[8] Farge M, Pellegrino G and Schneider K 2001 *Phys. Rev. Lett.* **87** 054501
[9] Kivotides D and Leonard A 2003 *Phys Rev. Lett.* **90** 234503
[10] Schekochihin A A, Cowley S C and Taylor S F 2004 *Astrophys. J.* **612** 276
[11] Tsinober A and Galanti B 2003 *Phys. Fluids* **15** 3514
[12] Llewellyn Smith S G and Tobias S M 2004 *J. Fluid Mech.* **498** 1
[13] Bigazzi A, Brandenburg A and Moss D 1999 *Phys. Plasmas* **6** 72
[14] Kivotides D and Leonard A 2004 *Europhys. Lett.* **65** 344
[15] Kivotides D and Leonard A 2004 *Europhys. Lett.* **66** 69
[16] Saffman P G 1992 *Vortex Dynamics* (Cambridge: Cambridge University Press)
[17] Schwarz K W 1988 *Phys. Rev.* B **38** 2398
[18] Kivotides D and Leonard A 2003 *Europhys. Lett.* **63** 354
[19] Chatelain P, Kivotides D and Leonard A 2003 *Phys. Rev. Lett.* **90** 054501
[20] Davidson P A 2004 *Turbulence: An Introduction for Scientists and Engineers* (Oxford: Oxford University Press)
[21] Ponty Y, Mininni P D, Montgomery D C, Pinton J-F, Politano H and Pouquet A 2005 *Phys. Rev. Lett.* **94** 164502
[22] Kazantsev A P 1968 *Sov. Phys.—JETP* **26** 1031
[23] Haugen N E L, Brandenburg A and Dobler W 2004 *Phys. Rev.* E **70** 016308
[24] Schekochihin A A, Boldyrev S A and Kulsrud R M 2002 *Astrophys. J.* **567** 828
[25] Tsinober A 2001 *An Informal Introduction to Turbulence* (Dordrecht: Kluwer)
[26] Kivotides D 2003 *Phys. Lett.* A **318** 574